Possible Role of Ultrasound in Assessment of Repaired Shoulder Joint

Shiamaa Samir Ahmed Ragab[1], Awad Abd-Elaziz Bessar[1], Essam Mohammed Hemat[1], Mohammed Abdella Abdelsalam[2]

1 Radiodiagnosis Department, Faculty of Medicine, Zagazig University, Egypt

2 Orthopedic Surgery Department, Faculty of Medicine, Zagazig University, Egypt

Email: shiamaaelwelily4@gmail.com, shelwalily@medicine.zu.edu.eg,

Article History: Received 10th June, Accepted 5th July, published online 10th July 2023

Abstract

Background: Ultrasound (US) imaging is an efficient, easy to use and inexpensive tool allowing for facilitated diagnosis and management of the painful shoulder. It remains primarily used by radiologists and rheumatologists, despite having shown excellent diagnostic accuracy when used by different medical specialities in their office-based consultation. It also has advantages over other imaging modalities in the evaluation of the postoperative shoulder for rotator cuff integrity and correct anchor and suture placement, as well as rotator cuff analysis following arthroplasty. Integration of US imaging into the orthopaedic surgeon's toolbox can be aided by a basic understanding of US principles, accompanied by a guide outlining basic techniques for evaluation of the healthy, pathological and postoperative shoulder as well as US-guided treatment possibilities.

Keywords: Ultrasound (US), Repaired Shoulder Joint

1. Introduction

Diagnostic ultrasound (US) is an undeniably helpful and essential resource in musculoskeletal medicine. Being rapid, accessible, dynamic, noninvasive, with rare side-effects and few demands on the patient, it has been widely integrated into the rheumatologist's and sport medicine physicians' toolbox [1,2]. Moreover, this investigation is relatively inexpensive. Parker et al. estimated that replacing magnetic resonance imaging (MRI) with US for the evaluation of specific shoulder pathology would save the United States $6.9 billion in health care costs between 2006 and 2020 [3]. The different specialists use US imaging to their advantage, for rapid analysis and diagnosis of easily accessible structures. It allows for office-based triage of lesions and pathologies, with those needing more in-depth investigation being sent on to radiology. When used as a guide, US also allows for more accurate joint injections, and is even advantageous over fluorosocopic guided joint injections [4,5]

2. Although it has a few disadvantages (being operator dependent with a relatively long learning curve and with little use in obese or severely limited mobility patients), it clearly has its place for use by the orthopaedic community as a first line diagnostic and treatment tool. Shoulder pain is a common complaint in an orthopaedic surgeon's consult. Finding what is responsible for the pain is evaluated through history taking, clinical examination, as well as further imagery. Rotator cuff lesions, although not solely responsible for the majority of shoulder pain, are often suspected, and their implication generally must be confirmed by further investigations, the choice of which is argued between US and MRI. It has been shown that US and MRI have comparable accuracy in

identifying fullthickness rotator cuff tears, and that US is accurate in predicting rotator cufftear reparability [2,6]. However, US seems to have lower accuracy compared to magnetic resonance arthrography (MRA) for measuring these rotator cuff tears and differentiating between partial and fullthickness tears [2,6].Whentaking into account accuracy, cost, and safety, Roy et al.[7]found that US was the best option compared with MRI and MRA. Additionally, it has been shown that the diagnostic accuracy of US in the characterisation of partial- and full-thickness rotator cuff tears, as well as tendinopathy, is similar

whether done by a trained radiologist, sonographer or orthopaedic surgeon, and efficacy of rotator cuff tear determination is increased after the introduction of shoulder US [7,8]. These findings encourage its use as a first-line screening tool for suspected rotator cuff tears by the orthopaedic surgeon.

Many resources are available reviewing US examination of the shoulder. However, few authors discuss techniques of US imaging in the surgical shoulder. This article will briefly review healthy shoulder US before outlining pathological imaging and mostimportantly, post-operativefindings, in order for the orthopaedic surgeon to more easily integrate this useful tool into his or her consultation. 2. US characteristics of regularly encountered structures in the shoulder As more thoroughly outlined by Iagnocco [9], it is important to understand the basic principles of how US imaging works in order to accurately interpret images and be able to differentiate between not only healthy and pathological structures, but also between endogenous tissues and exogenous materials. US imaging is possible due to waves that are reflected and absorbed differently, depending on a tissue's density and the velocity of sound within it, giving the tissue its unique acoustic impedance value. These reflected waves are then translated into a black and white image. Structures that show as bright white images are termed hyperechoic (having a high percentage of reflection, for example bone), darker images are given by hypoechoic structures (having a low percentage of reflection) and structures shown by a black image are known to be anechoic (having little or no reflection, for example, liquid). It is therefore clear that all tissues and materials will have different appearances depending on their respective characteristics (Fig. 1).

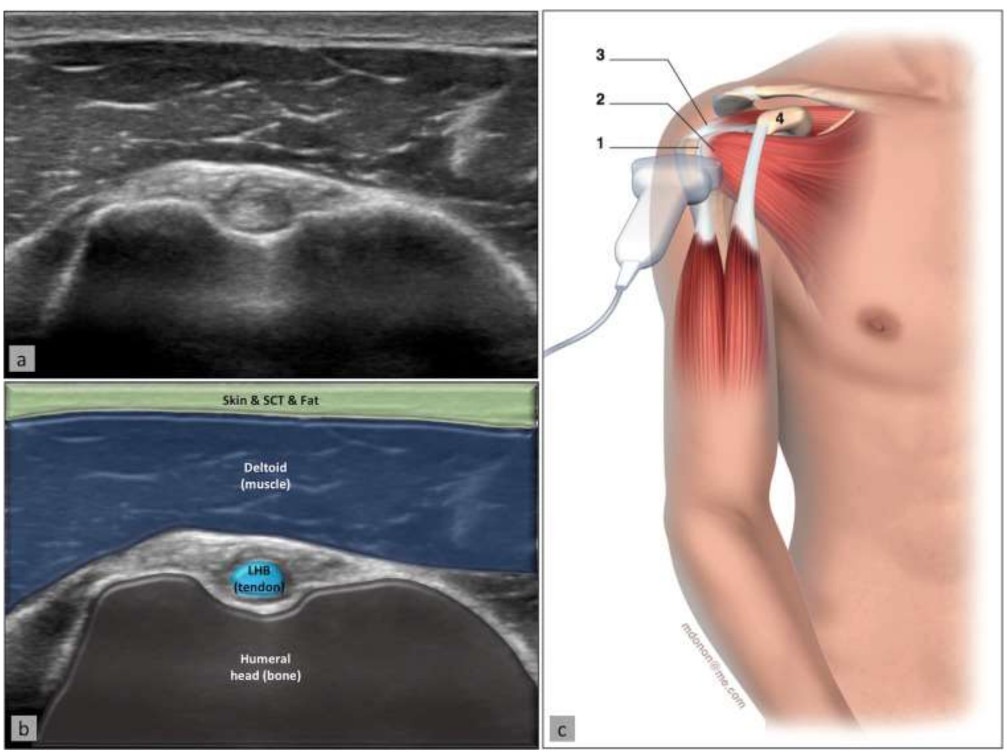

Fig. 1. Long head of the biceps tendon within the bicipital groove, visualised on its transverse axis. US image (a) with superimposed anatomy (b) and patient/probe position (c).

When a transducer is placed on a patient's shoulder, there must be direct contact with the skin, using gel to avoid an air gap, which would create an intense reflection and allowing little or no energy to penetrate for further imaging, due to the large difference of acoustic impedance between air and skin. Underneath the superficial hyperechoic skin layer lies the sub-cutaneous tissue, or fat, which is hypoechoic and contains a few hyperechoic striae of connective tissue, followed by muscle, also hypoechoic, and containing many either hyperechoic lines (on a longitudinal image) or hyperechoic dots (on a transverse image), representing the endomysium, perimysium and epimysium.

Some of the most important structures to analyse in the surgical shoulder are the rotator cuff tendons. On longitudinal images, these are seen as linear hyperechoic fibrillar patterns (only when perfectly perpendicular, avoiding anisotropy artefact), representing the endotendineal and peritendineal septa. It is important to differentiate between a tendon that is hypoechoic due to pathology or due to anisotropy.

Finally, the deepest anatomic structure visualised is bone, which produces a bright white image due to the large difference in acoustic impedance between it and soft-tissue, with very little (if no) energy continuing on. The same can be seen with calcifications within soft tissue, creating an anechoic shadow behind the calcification. Articular cartilage on the other hand, is seen as anechoic.

In the post-operative shoulder, different non-organic structures can be seen, such as sutures, anchors, metal, and certain plastics, each creating different effects. One such is shadowing, as seen with bone, when there is an absence of signal deeper to a hyperechoic structure. Sutures and polyethylene generate this sort of artefact due to the large impedance difference between them and the surrounding structures [10]. Another effect, this time encountered with metallic and glass objects, is the comet tail artefact, seen as hyperechoic bands deeper to the object, created by multiple internal reverberations occurring within these types of objects [11]. The last non-organic objects likely to be encountered in the postoperative shoulder are anchors, composed primarily of metal, polyether ether ketone (PEEK), polylactic acid but also calcium triphosphate [12]. These can have various aspects depending on the exact composition but are generally highly anisotropic, and are therefore difficult to see; as already mentioned, metal creates a comet tail artefact, as does polyactic acid and calcium triphosphate, while PEEK is much less visible, creating (when visible) a hyperechoic image of multiple aligned dots.

3. Basic examination of the healthy shoulder

US examination of the shoulder should be carried out using a systematic approach, analysing structures sequentially. The easiest position in which to carry out the entire examination is having the patient sitting on a seat with no backrest, in order to be able to have posterior access for the probe and to be able to move the shoulder in all directions [13]. As examiner, one can be standing or sitting, depending on personal preference. The various structures to be examined, the objectives as well as patient and probe positioning are outlined below.

3.1. Long head of the biceps tendon (LHB)

When examining the biceps tendon, place the patient's arm and probe as depicted in Fig. 1. This will allow transverse visualisation of the biceps tendon as well as its internal structure, to ensure that it lies within the bicipital groove and that there is no excess fluid surrounding it. Chang et al. suggest that <1 mm of fluid being normal while >3 mm is a severe effusion [14]. Anisotropy can be avoided by ensuring the probe is perpendicular to the tendon. The probe can then be rotated by 90 degrees in order to examine the tendon on its long axis, to ensure its integrity (Fig. 2).

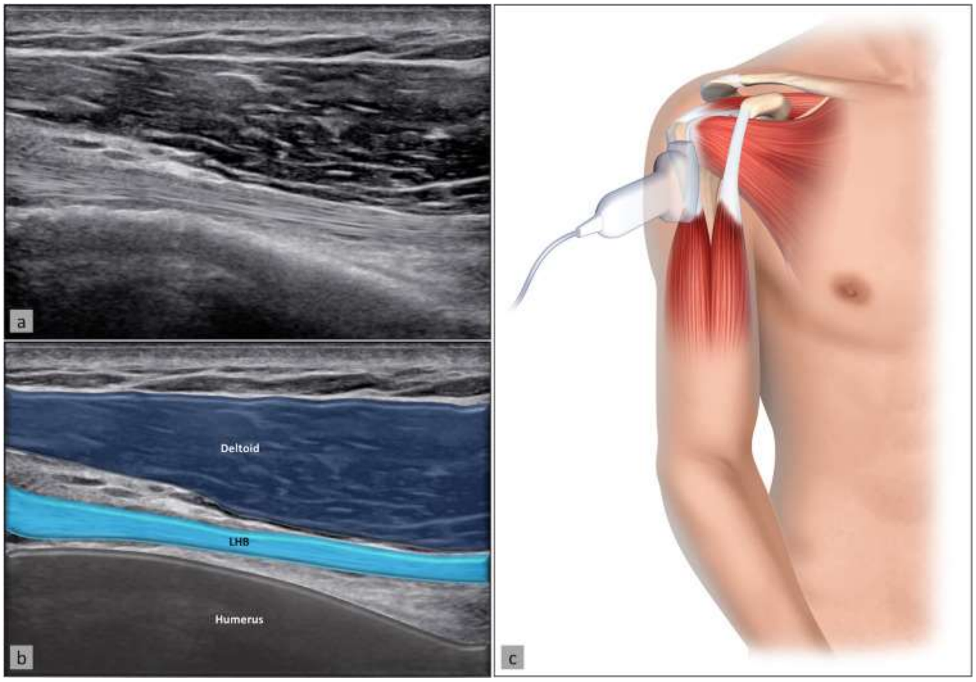

Fig. 2. Long head of the biceps tendon, visualised on its longitudinal axis. US image (a) with superimposed anatomy (b) and patient/probe position (c).

3.2. Subscapularis tendon and coracoid process

The subscapularis tendon, which inserts on the medial border of the bicipital groove and is a large group of tendons (8 cm superiorly to inferiorly) coming from a mutltipennate muscle, is best visualised with the shoulder in external rotation, elbow kept firmly by the thorax (Fig. 3), drawing the tendon out from beneath the coracoid process. While looking at the tendon's long axis, its integrity can be analysed, as well as its relationship with surrounding structures by dynamically performing internal and external rotation of the shoulder. Examination of the short axis of the tendon (by rotating the probe by 90 degrees) reveals its multifascicular pattern, and allows complete analysis from its upper border (with the biceps tendon lying supero-laterally), where injuries often begin, to its lower border.

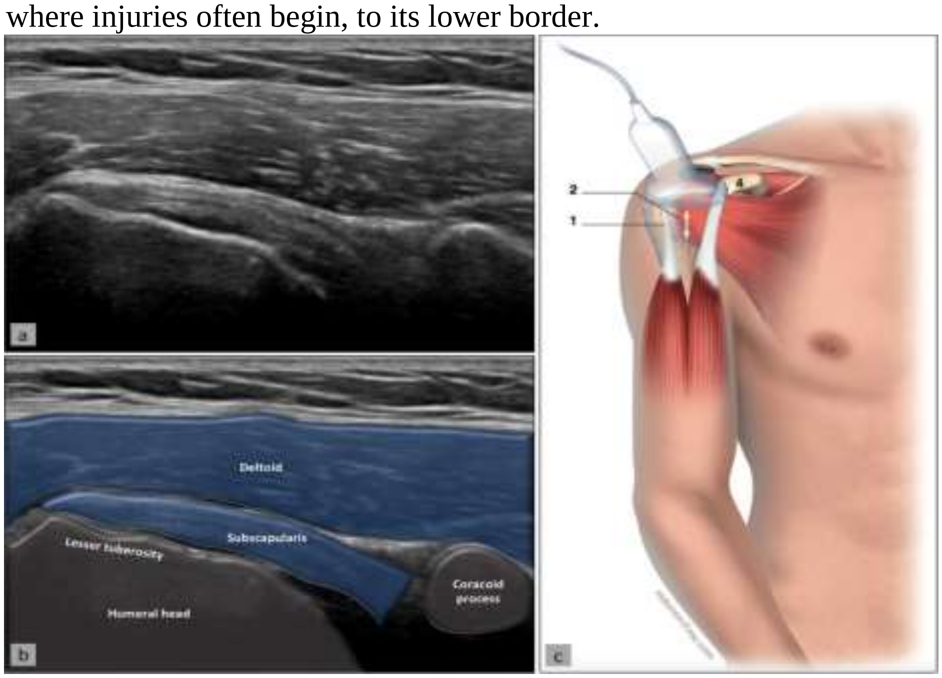

Fig. 3. Subscapularis tendon, visualised on its longitudinal axis. US image (a) with superimposed anatomy (b) and patient/probe position (c). Moving the probe cranio-caudally will allow for full analysis of the tendon.

3.3. Rotator cuff interval

The space through which the LHB passes as it leaves the glenohumeral joint is called the rotator cuff interval. The patient position is the same as for evaluation of the LHB, with the probe being placed slightly superiorly to the bicipital groove and in the axial plane (Fig. 4). The LHB is thus visualised with the subscapularis medially and the supraspinatus laterally, while the coracohumeral and superior glenohumeral ligaments surround it.

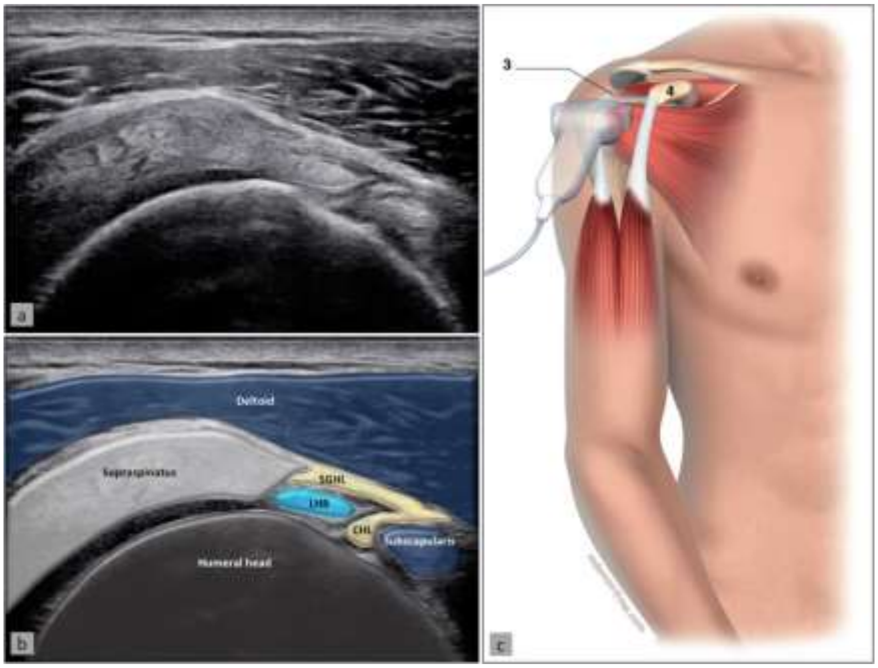

Fig. 4. Rotator cuff interval, containing the long head of the biceps, with a longitudinal view of the subscapularis medially and transverse view of the supraspinatus laterally, while the coracohumeral and superior glenohumeral ligaments surround it. US image (a) with superimposed anatomy (b) and patient/probe position (c).

3.4. Supraspinatus tendon and subacromial-subdeltoid bursa

The supraspinatus tendon is best visualised with the shoulder in abduction and internal rotation, by asking the patient to place the palm of their hand on their back pocket, elbow pointed backwards (Fig. 5). In patients presenting with reduced range of motion (adhesive capsulitis for example), maximal internal rotation with the arm hanging by the side of the thorax can be sufficient. The long axis of the tendon is most useful for analysing integrity of the tendon on the footprint (measuring approx. 2 cm medially to laterally), and is visualised by holding the probe in a tilted position (therefore not a true coronal plane but at an approx. 45 degree angle, following the line of the humerus–Fig. 5). This position also allows visualisation of two other structures: the subacromial-subdeltoid bursa (and the presence of excessive liquid, see below) and the humeral head along with its articular cartilage (and possible surface defects). In the axial plane (again not truly axial but at 90 degrees to the previous plane), the leading edge of the supraspinatus can be identified laterally to the biceps tendon. Moving the probe laterally will reveal the midportion of the tendon, with the anterior part of the infraspinatus eventually coming into view as an anisotropic and dark image (as the fibres run in a different plane).

Rotator Cuff Tears

The rotator cuff can present partial- or full-thickness tears, the former having no communication between the glenohumeral joint and the subacromial-subdeltoid bursa while the latter does [11]. Recognising these tears on US images can be difficult, and there are various signs that can aid in their recognition (Fig.5,), outlined in the table below (Table 2). Diagnosing incomplete tears can be particularly challenging if they are partially or completely shielded by bony structures (acromion) [15]. Normal supraspinatus tendon thickness evaluated by US (Fig. 5), varies between 4.4–5.75 mm [16], [17], [18], [19]. This variability is probably due to lack of standardisation of examiner position as well as transducer, recording and measurement parameters, and differences in population and their health status [17]. Injured supraspinatus tendon thickness documented by MRI has been found to be 5.4 ± 1.3 mm [20]. Any doubt concerning tendon tears should of course be further investigated by MRA. A suspraspinatus thickness above 9 mm is suspicious of a Fosbury lesion [21], [22].

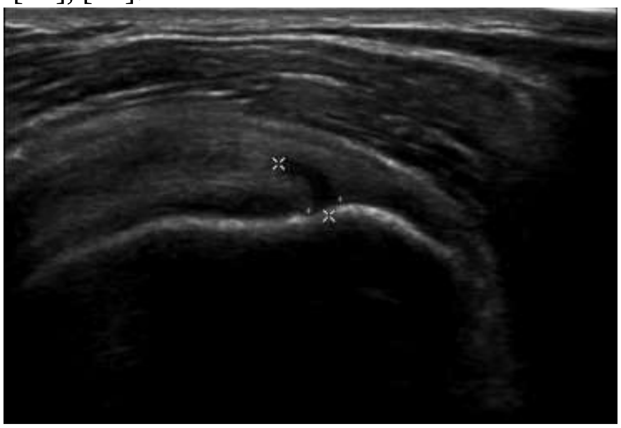

Fig.5. Supraspinatus partial thickness tear: anechoic tendon changes, focal tendon thinning.

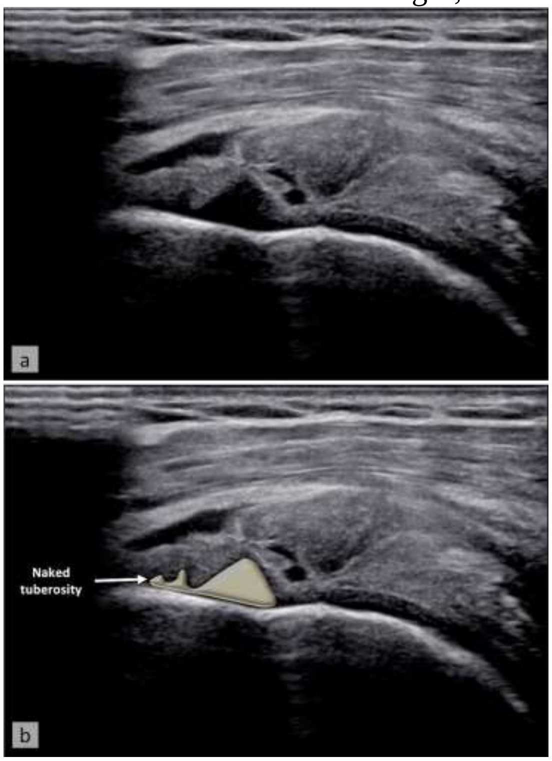

Fig. 6. Supraspinatus full thickness tear: naked tuberosity. US image (a) with superimposed anatomy (b).

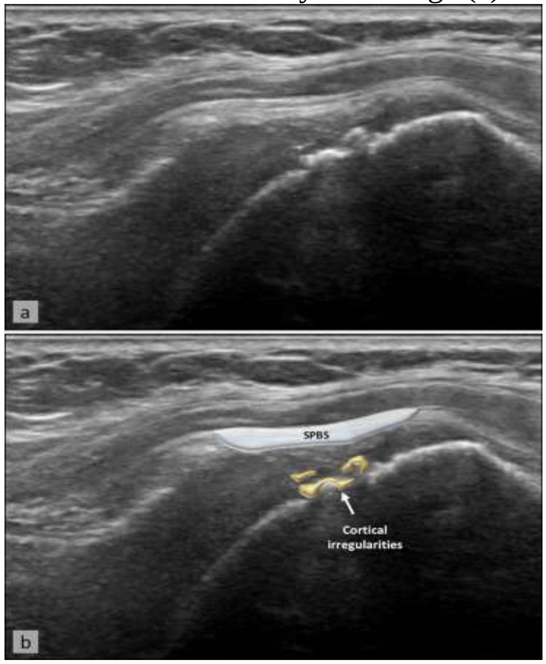

Fig. 7. Supraspinatus full thickness tear: "sagging peribursal fat sign" and cortical irregularities. US image (a) with superimposed anatomy (b).

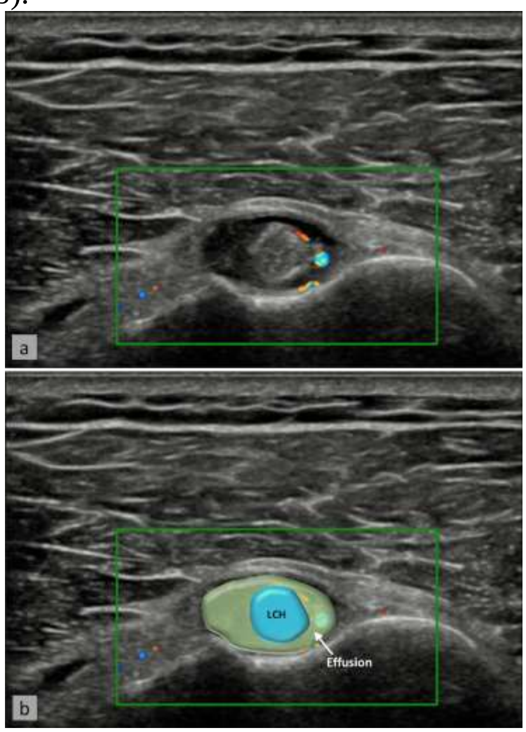

Fig. 8. Effusion surrounding the long head of the biceps, an indirect sign of rotator cuff pathology. US image (a) with superimposed anatomy (b).

Analysis of the rotator cuff muscles is important before determining indications for operative repair of the rotator cuff tendons. Muscle atrophy is not always easy to evaluate using US and requires expertise, but can be visualised by comparing the rotator cuff muscle to the surrounding muscles (for example, the deltoid) in regards to its bulk and reflectivity, and by analysing the central tendon, as fatty atrophy absorbs the US beam more than muscle tissue therefore blurring the margins of the central tendon and of the muscle itself [23], [24]. Additionally, because of the atrophy, fibrofatty septa become closer and therefore more prominent, and superficial muscles can create an indentation in atrophied muscles (Fig. 9) [11]. Wall et al. [24], having found the diagnostic performance of US to be comparable with that of MRI, propose a three-point grading scale for rotator cuff muscle atrophy

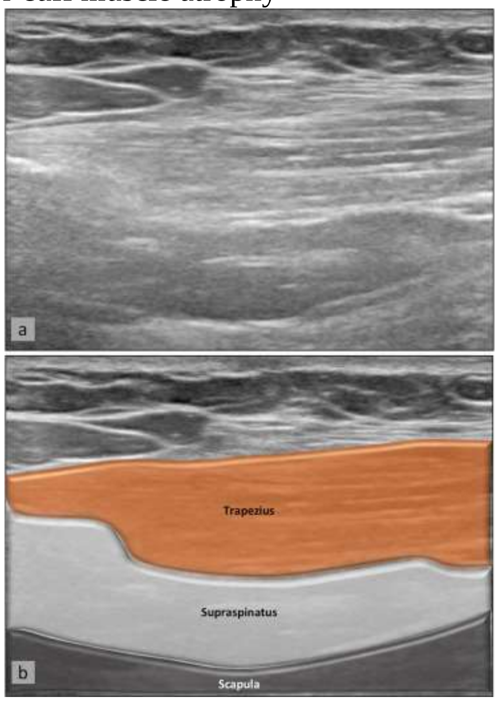

Fig. 9. Supraspinatus muscle atrophy, grade 2. The supraspinatus muscle is hyperechoic, with no discernible intramuscular tendon or muscle pennate pattern, in comparison with the trapezius and deltoid muscles visualised superficially. US image (a) with superimposed anatomy (b).

4.2. Calcifying tendinopathy

Calcific deposits can be recognised on US images as hyperechoic structures within the body of a tendon (Fig. 10). Although US can aid in localising these calcifications, it cannot identify and differentiate between the various phases; however, large calcific deposits, showing positive power Doppler signal and provoking subacromial-subdeltoid bursal reactions, have shown to be associated with shoulder pain [25], [26].

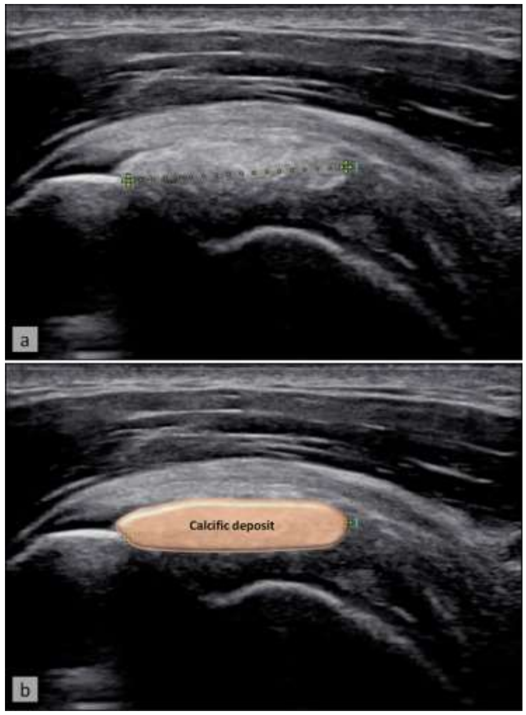

Fig. 10. Calcific deposit within the supraspinatus tendon, visualised as a hyperechoic structure within the body of the tendon. US image (a) with superimposed anatomy (b).

4.3. Subacromial-subdeltoid bursopathy

Thickening and distension of the subacromial-subdeltoid bursa can be a sign of different pathologies. To the best of our knowledge, there has yet to be an accurate definition of subacromial bursopathy on US. Normal bursal fluid thickness has been proposed but varies greatly, depending on whether the peribursal fat tissue is included, and due to the intra- and intervariability associated with US as discussed above. It is generally measured using as a landmark the hypoechoic strip within a hyperechoic layer of peribursal fat, located between the deltoid muscle and supraspinatus tendon (Fig. 5), and can range from 0.66 mm to 2 mm in normal conditions [17], [18], [19], [27], [28]. The only criterion for bursopathy published to date, using MRI, appears to be by White et al. [29], who define an abnormal amount of liquid in the subacromial-subdeltoid bursa to be present when the bursa fluid thickness is superior to 3 mm. This abnormal amount of liquid can result from full thickness rotator cuff tears, creating communication between the glenohumeral joint space and the subacromial-subdeltoid bursa, and from irritation of the bursa due to subacromial impingement [29]. These entities can therefore be considered local bursal reactions and not true inflammatory bursitis, which is due to other entities such as certain rheumatological diseases, crystal deposit, infection or haemorrhage [30], [31]. Thickening of the bursa synovial lining is also a sign of bursal reaction or true inflammation, and like effusion, there is no normal range defined for thickness, although a difference between both shoulders of over 2 mm has been proposed to be significant [13]. Thickening can also be seen as “bunching”, described below. By what has been described thus far in the literature, we can suggest a definition of bursopathy as being a subacromial-subdeltoid bursa measuring more than 3 mm or showing a difference of more that 2 mm compared to the healthy shoulder.

4.4. Impingement

There are numerous types of impingement syndromes, each having various aetiologies and consequences [32], [33]. Visualising the impingement itself through dynamic analysis is more challenging and requires more expertise

The most common is subacromial impingement, due to anatomical shape, os acromialis or acromioclavicular joint osteophytes [34]. Dynamic analysis involves abduction of the shoulder during imaging. Four signs have been described, including “bunching” of the subacromial-subdeltoid bursa or of the supraspinatus tendon beneath the acromium, “bulging” of the acromioclavicular ligament, and rarely “blocking” of the supraspinatus tendon [35].

Posterior internal impingement occurs often in overhead athletes and involves pinching of the supra- and infraspinatus tendons with the posterosuperior portion of the glenoid labrum when the shoulder is in abduction/external rotation/hyperextension [33]. Dynamic imaging of this pathological impaction is carried out with the patient's arm adducted and making external and internal rotation movements (Fig. 11) [36].

Fig. 11. Posterior impingement can be suspected when a partial thickness lesion of the articular surface of the infraspinatus tendon (arrow) is associated with cortical erosions of the humeral head (arrow head). US image (a) with superimposed anatomy (b). Adapted from Pesquer et al. [36].

A less common type of impingement concerns the subscapularis tendon during its passage between the coracoid and humeral head [36]. As with subacromial impingement, this can be dynamically visualised by internally rotating the shoulder when in position 2, revealing thickening and even snapping of the subcoracoidal bursal tissue [23], [24], as well as narrowing of the coracohumeral interval [24].

4.5. Acromioclavicular joint arthropathy

Acromioclavicular joint pathology is relatively easy to analyse using US imaging. Pathological signs can be detected (osteophytes, erosions, effusion and geyser phenomenon, being a large synovial cyst extending into the supraclavicular fossa) and joint tenderness evaluated by applying pressure on the probe whilst above the joint line [24]. Dynamic analysis (the patient's arm being brought from neutral position to a “cross arm” position) can reveal joint subluxation [37].

4.6. Fractures

US has shown to have comparable sensitivity and specificity to x-ray for the diagnosis of fractures following acute trauma, and in particular humeral fractures (sensitivity of 76.2%) [38], [39], [40]. It can therefore be useful in identifying subtle greater tuberosity fractures that have gone undiagnosed.

5. Joint injections

In the shoulder, there are three spaces in which joint injections can be done, and these are facilitated by US guiding [4], [5], especially when using cortisone as its entry into whichever space is seen as hyperechoic particles, ensuring accurate placement of the medication. The needle is generally inserted in the same plane as the probe, allowing for it to be followed until reaching the area needed to be injected. The specific techniques will not be outlined in this article.

The most common is in the subacromial bursa, with the patient being in position 3, and injection of the liquid is easily visualised as the bursa inflates The acromioclavicular joint space can also benefit from joint injection, with easy visualisation of the needle within the joint space. Lastly, glenohumeral joint injection, carried out posteriorly in position 4, can be more challenging, especially in patients with excess adipose tissue, as the structures are deeper. It is important to visualise the posterior glenoid and labrum medially and the humerus laterally, in order to correctly insert the needle into the intra-articular space (Fig. 18). Two paramount signs to know that one is within the joint capsule is the disappearance of the injected liquid into the joint, and the lack of resistance when injecting the liquid [13].

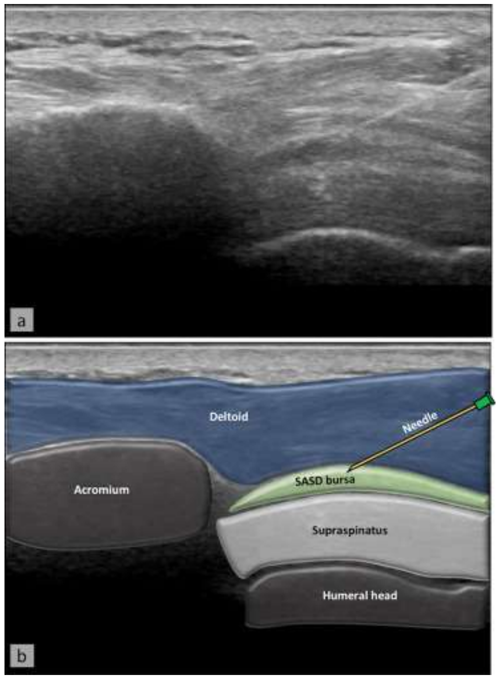

Fig. 12. Subacromial-subdeltoid bursa joint injection. The needle is inserted at the mid-line of the lateral edge and parallel to the probe, allowing it to be visualised entering the subacromial-subdeltoid bursa. US image (a) with superimposed anatomy (b).

6. The surgical shoulder

US imaging is a useful tool for analysing the post-operative shoulder, particularly following rotator cuff reparation. US classification of rotator cuff integrity has shown some prognostic value, aiding in prediction of postoperative shoulder function [15]. It can also reassure patients with persistent pain as to adequate tendon healing, and if it is not the case, diagnose complications such as anchor displacement or recurrent tear; for this use, US has shown similar statistical strength as MRI, and even has certain advantages over MRI, on which a recurrent tear can be difficult to diagnose due to repaired tendons showing persistent altered signals for over 6 months due to tissue remodelling, liquid leakage from the glenohumeral to the subacromial space being normal after surgery (opening of the rotator interval and passage of instruments through the tendons) and foreign structures creating considerable artefacts [42]. Additionally, before deciding whether a surgical revision is necessary, the quality of the bone, tendon and muscle can be evaluated.

Post-operative tendons have been described as being hypoechoic with an absence of the normal fibrillar pattern, as well as showing peritendinous vascularity (the tendon itself remaining relatively avascular), with these three characteristics normalising over a period of 6 months [43], [44]. Additionally, the supraspinatus tendon's anatomical footprint increases (7 mm to 9.3 mm) while its thickness has been shown to stay constant or decrease, being within a range of 4.3 mm to 5.75 mm, over the 6-12 month postoperative period [43], [44], [45]. Caution is proposed in patients showing postoperative US supraspinatus thickness of less than 4 mm with regards to activities of daily living and rehabilitation. Different aspects can also be present at the reinsertion zone, depending on the surgical technique used, such as persistent "sagging peribursal fat sign" of the repaired tendon insertion and hyperechoic modifications due to the presence of tendon reinforcement [34]. The Sugaya classification (Table 4), on the other hand, proposes sufficient tendon thickness to be >2 mm; this classification, the only one to date validated for US evaluation of tendon healing (originally developed for MRI), also takes into account tendon echostructure (echogenicity, heterogenicity, continuity) [15], [46]. Concerning the subacromial-subdeltoid bursa following rotator cuff repair (otherwise termed neo-bursa as subacromial-subdeltoid bursectomy is practically always carried out), it shows effusion and increased thickness, which also decreases over time (from 1.9 mm at 1 week to 0.7 mm at 6 months) [34], [45]

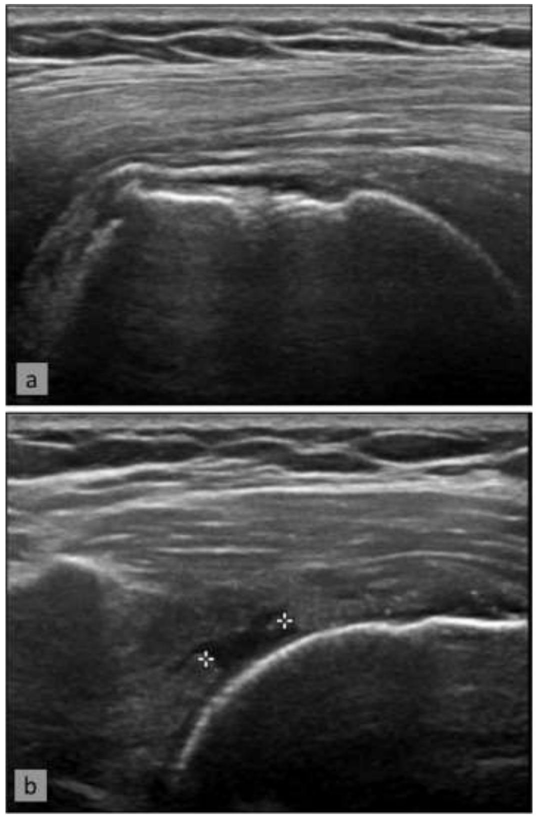

Fig. 13. Postoperative evaluation of rotator cuff repair using the Sugaya classification. A type III tendon shows insufficient thickness but does not show discontinuity (a), while in a type IV tendon there is the presence of a minor discontinuity, suggesting a small tear (b).

The appearance of anchors and sutures has already been discussed previously, in the section concerning US characteristics, and its analysis can be of particular interest in evaluating biodegradable suture and anchor displacement, an uncommon complication of rotator cuff repair (Fig. 14) [47].

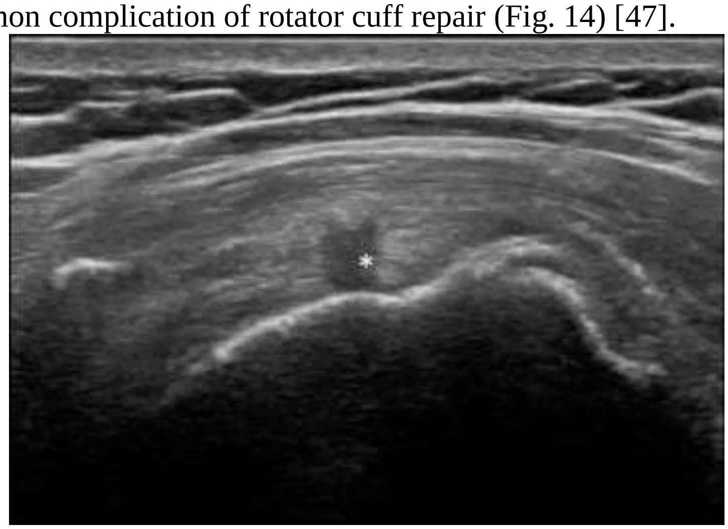

Fig. 14. Postoperative evaluation of rotator cuff repair, with visualisation of a suture and the posterior shadow it creates (*).

Rotator cuff analysis by US following arthroplasty, although rarely carried out, can also be of importance essentially for the subscapularis (Fig. 15). This tendon is a dynamic stabiliser of the humeral head, its failure therefore having an effect on shoulder strength and function; imaging cannot, however, differentiate between functional and non-functional structurally intact repairs [45]. US can also be useful for first-line evaluation of other complications such as infection of the prosthesis, visualised by intra- or juxta-articular effusion/liquid masses with hypervascularity on the Doppler, or migration of prosthetic fragments [34].

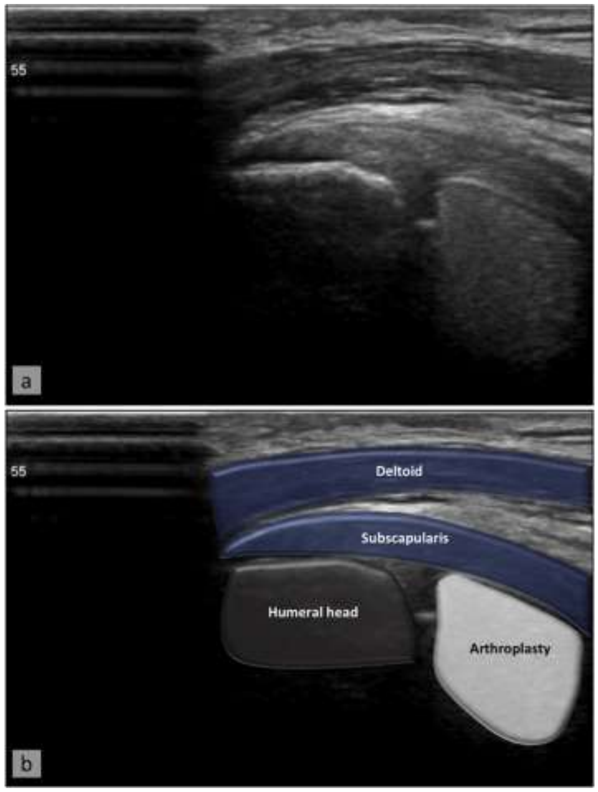

Fig. 15. Postarthrosplasty evaluation for the presence of effusion, hypervascularity, migration of prosthetic fragments, and of the rotator cuff tendons. US image (a) with superimposed anatomy (b).

US imaging is an excellent tool for evaluation of a painful shoulder, being easily accessible, rapid and inexpensive and causing little or no discomfort to the patient. It has uses not only for initial diagnoses, but also importantly for a surgeon, postoperative analysis, allowing earlier and more accurate recognition of complications and bringing prognostic value and reassurance to patients.

This work was following results the study was demonstrated by Plomb et al. [48] who assessed guide to ultrasound imaging of the postoperative rotator injured shoulder.

References

[1] Finnoff JT. The evolution of diagnostic and interventional ultrasound in sports medicine. PM and R. J Inj Funct Rehabil 2016;8:S133–8.
[2] Naqvi GA, Jadaan M, Harrington P. Accuracy of ultrasonography and magnetic resonance imaging for detection of full thickness rotator cuff tears. J Shoulder Surg 2009;3:94–7.
[3] Parker L, Nazarian LN, Carrino JA, Morrison WB, Grimaldi G, Frangos AJ, et al. Musculoskeletal imaging: medicare use, costs, and potential for cost substitution. J Am Coll Radiol 2008;5:182–8.
[4] Daley EL, Bajaj S, Bisson LJ, Cole BJ. Improving injection accuracy of the elbow, knee, and shoulder: does injection site and imaging make a difference? A systematic review. Am J Sports Med 2011;39: 656–62.
[5] Rutten MJ, Collins JM, Maresch BJ, Smeets JH, Janssen CM, Kiemeney LA, et al. Glenohumeral joint injection: a comparative study of ultrasound and fluoroscopically guided techniques before MR arthrography. Eur Radiol 2009;19:722–30.
[6] Tse AK, Lam PH, Walton JR, Hackett L, Murrell GA. Ultrasound determination of rotator cuff tear repairability. Shoulder Elbow 2016;8:14–21.
[7] Roy JS, Braen C, Leblond J, Desmeules F, Dionne CE, MacDermid JC, et al. Diagnostic accuracy of ultrasonography MRI and MR arthrography in the characterisation of rotator cuff disorders: a systematic review and meta-analysis. Br J Sports Med 2015;49:1316–28.
[8] Chiu CH, Chen P, Chen AC, Hsu KY, Chang SS, Chan YS, et al. Shoulder ultrasonography performed by orthopedic surgeons increases efficiency in diagnosis of rotator cuff tears. J Orthop Surg Res 2017;12:63.
[9] Iagnocco A. Textbook on musculoskeletal ultrasound in rheumatology. BMJ Books; 2016.
[10] Bianchi S, Martinoli C. Ultrasound of the musculoskeletal system. Berlin Heidelberg: Springer-Verlag 2007.
[11] van Holsbeeck M, Introcaso J. Musculoskeletal ultrasound. 3rd ed. New Delhi: Jaypee Brothers Medical Pub; 2016.
[12] Collin P, Lädermann A. Instrumentation, matériaux et sutures en chirurgie arthroscopique de l'épaule. L'arthroscopie 2015.
[13] McNally E. E-B. Practical musculoskeletal ultrasound. 2nd ed. Elsevier Health Sciences; 2014. p. 2014.
[14] Chang KV, Chen WS, Wang TG, Hung CY, Chien KL. Associations of sonographic abnormalities ofthe shoulder with various grades of

biceps peritendinous effusion (BPE). Ultrasound Med Biol 2014;40:313–2

[15] Barth J, Fotiadis E, Barthelemy R, Genna S, Saffarini M. Ultrasonic evaluation of the repair integrity can predict functional outcomes after arthroscopic double-row rotator cuff repair. Knee Surg Sports Traumatol Arthrosc 2015;23: 376–85.

[16] AkturkM,KaraahmetogluS,KacarM,Muftuoglu O. Thickness ofthe supraspinatus and biceps tendons in diabetic patients. Diabetes care 2002;25:408.

[17] Hougs Kjaer BPM, Ellegaard KPP, Wieland IP, Warming SPP, Juul-Kristensen BPP. Intra-rater and inter-rater reliability of the standardized ultrasound protocol for assessing subacromial structures. Physiother Theory Pract 2017;33:398–409.

[18] Kim K, Kim HG, Song D, Yoon JY, Chung ME. Ultrasound dmensions of the rtator cuff and other associated structures in korean ealthy adults. J Korean Med Sci 2016;31:1472–8.

[19] Ohya N, Yamada T, Satoh Y, Kawamura H. Relative and absolute reliability of ultrasound measurements for the thickness of the soft tissue around the shoulder joint of young normal subjects. J Phys Ther Sci 2017;29: 754–9.

[20] Kolts I, Busch LC, Tomusk H, Rajavee E, Eller A, Russlies M, et al. Anatomical composition ofthe anterior shoulder joint capsule.Acadaver study on 12 glenohumeral joints. Annals of anatomy =Anatomischer Anzeiger: official organ of the Anatomische Gesellschaft 2001;183:53–9.

[21] Kolo FC, Schwitzguebel AJ, Kourhani A, Denard PJ, Charbonnier C, Ladermann A. Fosbury flop tear of the rotator cuff: diagnostic asessment with mgnetic rsonance athrography. J Radiol 2017:20170146.

[22] Lädermann A, Denard PJ, Kolo FC. A new tear pattern of the rotator cuff and its treatment: Fosbury flop tears. J Shoulder Surg 2015;9:9–12.

[23] Tracy MR, Trella TA, Nazarian LN, Tuohy CJ, Williams GR. Sonography of the coracohumeral interval: a potential technique for diagnosing coracoid impingement. J Ultrasound Med 2010;29:337–41.

[24] Wall LB, Teefey SA, MiddletonWD, Dahiya N, Steger-May K, Kim HM, et al. Diagnostic performance and reliability of ultrasonography for fatty degeneration of the rotator cuff muscles. J Bone Joint Surg Am 2012;94:e83.

[25] Farin PU, Jaroma H. Sonographic findings of rotator cuff calcifications. J Ultrasound Med 1995;14:7–14.

[26] Le Goff B, Berthelot JM, Guillot P, Glemarec J, Maugars Y. Assessment of calcific tendonitis of rotator cuff by ultrasonography: comparison between symptomatic and asymptomatic shoulders. Joint Bone Spine 2010;77: 258–63.

[27] Karthikeyan S, Rai SB, Parsons H, Drew S, Smith CD, Griffin DR. Ultrasound dimensions of the rotator cuff in young healthy adults. J Shoulder Elbow Surg 2014;23:1107–12.

[28] van Holsbeeck M, Strouse PJ. Sonography of the shoulder: evaluation of the subacromial-subdeltoid bursa. AJR Am J Roentgenol 1993;160:561–4.

[29] White EA, Schweitzer ME, Haims AH. Range of normal and abnormal subacromial/subdeltoid bursa fluid. J Comput Assist Tomogr 2006;30:316–20. [30] Awerbuch MS. The clinical utility of ultrasonography for rotator cuff disease, shoulder impingement syndrome and subacromial bursitis. Med J Aust 2008;188:50–3.

[31] Ishii H, Brunet JA, Welsh RP, Uhthoff HK. “Bursal reactions” in rotator cuff tearing, the impingement syndrome, and calcifying tendinitis. J Shoulder Elbow Surg 1997;6:131–6.

[32] Cunningham G, Lädermann A. Redefining anterior shoulder impingement: a literature review. Int Orthop 2017.

[33] Lädermann A, Chague S, Kolo FC, Charbonnier C. Kinematics of the shoulder joint in tennis players. J Sci Med Sport 2016;19:56–63.

[34] Brasseur J, Jakob B. Echographie de l’épaule et de la paroi thoracique. Sauramps Médical; 2014.

[35] Read JW, Perko M. Ultrasound diagnosis of subacromial impingement for lesions of the rotator cuff. Australas J Ultrasound Med 2010;13:11–5.

[36] Pesquer L, Poussange N,Moreau-DurieuxM,Meyer P, LädermannA,Abadie P. Le conflit postérosupérieur de l’épaule. In: Acutalité en échographie. Montpellier: Sauramps Médical; 2017.

[37] de Beer J, Bhatia DN. Shoulder sonography: Diagnostic and interventional utility. Int J Shoulder Surg 2010;4:51–4.

[38] Bozorgi F, Shayesteh Azar M, Montazer SH, Chabra A, Heidari SF, Khalilian A. Ability of ultrasonography in detection of different extremity bone fractures; a case series study. Emerg (Tehran) 2017;5:e15.

[39] Joshi N, Lira A, Mehta N, Paladino L, Sinert R. Diagnostic accuracy of history, physical examination, and bedside ultrasound for diagnosis of extremity fractures in the emergency department: a systematic review. Acad Emerg Med 2013;20:1–15.

[40] Schmid GL, Lippmann S, Unverzagt S, Hofmann C, Deutsch T, Frese T. The investigation of suspected fracture-a comparison of ultrasound with conventional imaging. Dtsch Arztebl Int 2017;114:757–64.

[41] De Conti G, Marchioro U, Dorigo A, Boscolo N, Vio S, Trevisan M, et al. Percutaneous ultrasound-guided treatment of shoulder tendon calcifications: Clinical and radiological follow-up at 6 months. J Ultrasound 2010;13:188–98.

[42] Collin P, Yoshida M, Delarue A, Lucas C, Jossaume T, Lädermann A, et al. Evaluating postoperative rotator cuff healing: Prospective comparison of MRI and ultrasound. Orthop Traumatol Surg Res 2015;101:S265–8.

[43] Cadet ER, Adler RS, Gallo RA, Gamradt SC, Warren RF, Cordasco FA, et al. Contrast-enhanced ultrasound characterization of the vascularity of the repaired rotator cuff tendon: short-term and intermediate-term follow-up. J Shoulder Elbow Surg 2012;21:597–603.

[44] Yoo HJ, Choi JY, Hong SH, Kang Y, Park J, Kim SH, et al. Assessment of the postoperative appearance of the rotator cuff tendon using serial sonography after arthroscopic repair of a rotator cuff tear. J Ultrasound Med 2015;34:1183–90.

[45] Tham ER, Briggs L, Murrell GA. Ultrasound changes after rotator cuff repair: is supraspinatus tendon thickness related to pain? J Shoulder Elbow Surg 2013;22:e8–15.

[46] Sugaya H, Maeda K, Matsuki K, Moriishi J. Repair integrity and functional outcome after arthroscopic double-row rotator cuff repair. A prospective outcome study. J Bone Joint Surg Am 2007;89:953–60.

[47] Oh J, Song B, Rhie T-Y. Two cases of biodegradable suture anchor displacement diagnosed with ultrasonography following arthroscopic rotator cuff repair. Clin Shoulder Elbow 2015;18:254–60.

[48] Plomb-Holmes C, Clavert P, Kolo F, Tay E, Lädermann A; French Arthroscopic Society. An orthopaedic surgeon's guide to ultrasound imaging of the healthy, pathological and postoperative shoulder. Orthop Traumatol Surg Res. 2018;104(8S):S219-S232. doi:10.1016/j.otsr.2018.07.011